University of Nebraska - Lincoln

DigitalCommons@University of Nebraska - Lincoln

David Sellmyer Publications

Research Papers in Physics and Astronomy

January 1995

Electronic structures and Curie temperatures of iron-based rare-earth permanent-magnet compounds

J.P. Woods
University of Nebraska - Lincoln

B.M. Patterson
University of Nebraska - Lincoln

A.S. Fernando
University of Nebraska - Lincoln

Sitaram Jaswal
University of Nebraska, sjaswal1@unl.edu

D. Welipitiya
University of Nebraska - Lincoln

See next page for additional authors

Follow this and additional works at: https://digitalcommons.unl.edu/physicssellmyer

Part of the Physics Commons

Authors

J.P. Woods , B.M. Patterson, A.S. Fernando, Sitaram Jaswal, D. Welipitiya, and David J. Sellmyer

Electronic structures and Curie temperatures of iron-based rare-earth permanent-magnet compounds

J. P. Woods, B. M. Patterson, A. S. Fernando, S. S. Jaswal, D. Welipitiya, and
D. J. Sellmyer

*Behlen Laboratory of Physics and Center for Materials Research and Analysis, University of Nebraska,
Lincoln, Nebraska 68588*

The modification of the electronic structures of $Sm_2Fe_{17-x}Al_xN_y$, $NdFe_{11}TiN_y$, and $YFe_{12-x}Mo_x$ upon alloying and nitriding are examined with self-consistent spin-polarized calculations and soft-x-ray photoemission measurements between 18 and 135 eV. The changes in the Curie temperature T_c with substitutional modifications and nitrogen addition are modeled with self-consistent spin-polarized electronic structure calculations and the spin-fluctuation theory of Mohn and Wohlfarth which relates the electronic structure to T_c. The calculations show that the spin-summed density of states at the Fermi energy is related to T_c. The photoemission spectra are dominated by the Fe 3d electrons within 3 eV of the Fermi energy in agreement with calculations. Changes in the density of states at the Fermi energy for interstitial and substitutional modification compare well with calculations. Using photoemission results with experimental magnetic moments for the substitutional modification of the compound $Sm_2Fe_{17-x}Al_x$, the spin-fluctuation theory predicts a change in T_c in agreement with the measured change in T_c. Spin-resolved photoemission spectra for c-axis oriented $Sm_2Fe_{17}N_{2.6}$ with magnetization perpendicular to the surface are presented and compared to theoretical calculations.

I. INTRODUCTION

The magnetic properties required for permanent magnetic materials are large magnetization, large uniaxial magnetic anisotropy, and high Curie temperature (T_c). Since the 1960s, superior magnetic materials are compounds of light rare-earth elements (R) and ferromagnetic transition metals (T).[1] The R-T compounds have a large magnetization due to the high T concentration and a large magnetic anisotropy due to the anisotropic crystal structure and large single-ion anisotropy associated with non-s-state rare earths. The first R-T compound to attain widespread application was $SmCo_5$ having the $CaCu_5$ structure.[2] The SmCo-based materials are inherently expensive due to the high cost of the raw materials. Iron-based R-T compounds are less expensive but compounds with larger Fe concentrations have lower T_c values.[3] Initial work with rapidly quenched R-T systems alloyed with boron led to the discovery of the ternary crystalline compound $Nd_2Fe_{14}B$ (Ref. 1) with $T_c = 585$ K.

Coey and co-workers[4] recently have shown that interstitial nitrogen addition to the R_2Fe_{17} compounds increases T_c by as much as 400 K. The R_2Fe_{17} compounds have planar magnetic anisotropy for all the rare earths, and only the compound $Sm_2Fe_{17}N_{2.6}$ has a uniaxial magnetic anisotropy. The nitrided iron-rich compound $Sm_2Fe_{17}N_{2.6}$ with $T_c = 743$ K is being developed for permanent-magnet applications.

The R-Fe compounds can also be modified with partial substitution, for example, Al for Fe in the compound $Sm_2Fe_{17-x}Al_x$.[5-8] Interestingly, T_c increases for Al substitution for values of x up to 3 while the magnetiza-

tion per formula unit decreases. Partial substitution of a non-magnetic transition metal (M) for Fe stabilizes the $RFe_{12-x}M_x$ structure in the $ThMn_{12}$ structure. The 2:17 and 1:12 structures are closely related as slight modifications of the $CaCu_5$ hexagonal structure.[9] In considering possible compounds for examining changes in T_c with M substitution, the compound $YFe_{12-x}Mo_x$ was selected because it exhibits a large decrease in T_c with increased Mo concentration[10] and the substitution site has been determined by x-ray diffraction.[11]

In this work we have investigated the mechanism for the drastic change in the T_c in the R-Fe compounds with interstitial addition and substitutional modification. Previous workers[6,10,12-14] have advocated a mean-field model to explain qualitatively the increase in T_c with lattice expansion. In Sec. II the inadequacies of this model are discussed and the spin-fluctuation theory of Mohn and Wohlfarth[15] is summarized. In Sec. III self-consistent, spin-polarized calculations of the electronic structure for several Fe-based compounds and quantitative comparisons of the theoretical and experimental change in T_c with modifications are presented. In Sec. IV the details of sample preparation, characterization, and photoemission results are presented and discussed. The conclusions of this work are summarized in Sec. V.

II. CURIE TEMPERATURE MODELS

Previous investigators have explained the variation of T_c with interstitial addition[12-14] and substitutional modification[6,10] with a mean-field model and an interatomic-distance-dependent exchange energy as represented by the Bethe-Slater curve. As noted by Herbst,[1]

"attributing T_c behavior solely to distance dependent exchange is undoubtedly an oversimplification." Although the distance-dependent exchange model does correlate the results of T_c variation in a wide variety of the compounds, there are several weaknesses of the model that must be considered: (1) Goodenough[16] has discussed the Bethe-Slater curve and concludes that the curve is incorrect. (2) T_c depends on the local coordination of the magnetic ions. In simple systems with one site, the theory is straightforward but with three or more Fe sites in the R-Fe compounds the effect of local coordination is complicated, especially with substitutional modifications. (3) As noted by Chen,[17] the mean-field model is an ionic model which applies well to the rare-earth elements but Fe-based compounds are clearly itinerant magnetic systems. (4) There are several compounds that do not exhibit an increase in T_c as the lattice constant increases. For the compound $YFe_{12-x}Mo_x$,[10] as x increases the lattice constant increases but T_c decreases. As a second example, a recent publication[18] has shown that for the Si-substituted compound $Ce_2Fe_{17-x}Si_x$, as x increases, the volume decreases, and the magnetic moment per formula unit decreases, but T_c increases. The mean-field model does have its merits, but the underlying mechanism that alters T_c in the modified R-Fe compounds is not readily apparent in the mean-field model of magnetism.

Mohn and Wohlfarth[15] have developed a model that considers the spin fluctuations of local atomic moments in determining T_c in itinerant electron systems. T_c is determined by the solution to the algebraic equation

$$\frac{T_c^2}{T_S^2} + \frac{T_c}{T_{SF}} - 1 = 0 , \qquad (1)$$

where T_S is the calculated Curie temperature based on the Stoner model of itinerant electron magnetism and T_{SF} is a characteristic temperature describing the influence of spin fluctuations. The calculated value of T_S is much larger than the measured T_c,[15] and T_c is determined primarily by the second term in Eq. (1). The spin-fluctuation temperature is given by[15]

$$T_{SF} = \frac{M_0^2}{10 k_B \chi_0} , \qquad (2)$$

where M_0 is the zero-temperature magnetic moment and k_B is Boltzmann's constant. χ_0 is the exchange-enhanced susceptibility and is given by[19]

$$\frac{1}{\chi_0} = \frac{1}{4\mu_B^2} \left(\frac{1}{N_\uparrow(E_F)} + \frac{1}{N_\downarrow(E_F)} - 2I \right) , \qquad (3)$$

where $N_\uparrow(E_F)$ and $N_\downarrow(E_F)$ are the up- and down-spin density of states at the Fermi energy and I is the Stoner parameter. The quantities M_0, χ_0, $N_\uparrow(E_F)$, $N_\downarrow(E_F)$, and I are directly determined by theoretical electronic structures.

III. THEORETICAL ELECTRONIC STRUCTURE

The electronic structures of Y_2Fe_{17} and $NdFe_{11}Ti$ parent compounds and their nitrides $Y_2Fe_{17}N_3$ and $NdFe_{11}TiN$ have been reported by Jaswal et al.[20,21]

The electronic structure is calculated using self-consistent spin-polarized calculations based on the linear-muffin-tin-orbital method in the scalar relativistic approximation.[22] The theoretical ratio $T_c(Y_2Fe_{17}N_3)/T_c(Y_2Fe_{17})$ based on the spin-fluctuating theory and the calculated density of states (DOS) is compared to the measured T_c ratio. The theoretical T_c ratio for the parent compound Y_2Fe_{17} (2.34) is within 9% of the experimental value (2.14).[20] For the $NdFe_{11}Ti$ compound, the calculated Curie temperature ratio (1.32) is within 1% of the experimental value (1.31).[21] The absolute T_c's are not correctly predicted by the spin-fluctuation theory using the calculated electronic structures, but the calculated relative changes in T_c's are in very good agreement with experiment.

The calculated DOS for $Y_2Fe_{17}N_3$ has been employed by Katter et al.[23] to determine the T_c of $Sm_2Co_{17}N_3$. The Fermi level is shifted to account for the additional $3d$ electron on Co and very little change in the spin-resolved DOS at the Fermi energy is interpolated from the calculated electronic structure.[20] In this case, T_c is independent of χ_0, and a reduced T_c in $Sm_2Co_{17}N_3$ is due to a reduction in the magnetic moment. The predicted T_c (834 K) is in very good agreement with the experimental value (811 K).

The spin-fluctuation theory is applied here to the substitutional modification of T_c in R-Fe compounds. The self-consistent spin-polarized electronic structure for $Y_2Fe_{12-x}Mo_x$ for $x = 1$ and 2 is shown in Fig. 1. The electronic structure is dominated by the Fe $3d$ bands near the Fermi energy, and an exchange splitting of about 2.0 eV is evident. There are only slight changes in the electronic structure as the Mo concentration increases from $x = 1$ to $x = 2$; the DOS at E_F changes less than 3% in both the up- and down-spin DOS. The calculated and measured zero-temperature magnetic moments are not in good agreement. The magnetic moment per formula unit (f.u.) from the calculations are $22.0\mu_B$/f.u. and
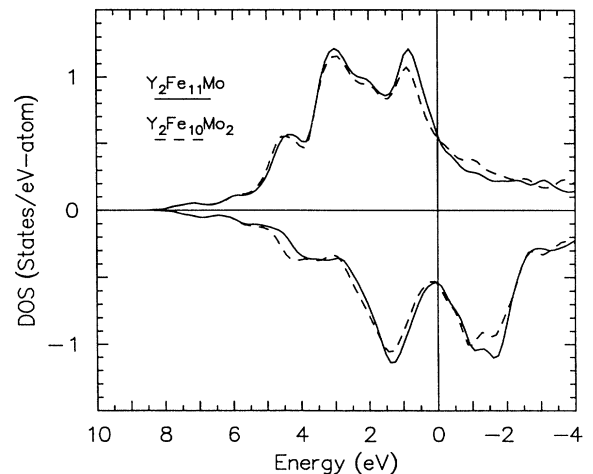

FIG. 1. Spin-polarized density of states for $YFe_{11}Mo$ (solid line) and $YFe_{10}Mo_2$ dashed line. The zero of energy represents the Fermi energy.

19.2μ_B/f.u. for $x = 1$ and 2, respectively. Experimentally the moments have been measured[10] as 23.7μ_B/f.u. and 14.1μ_B/f.u. for $x = 1$ and 2, respectively. The disagreement in the magnetic moment may be due to a noncollinear alignment of the moments in the compound and/or the inadequacies of representing the disorder of the Mo sites in the theoretical model.[21] Applying the spin-fluctuation model with the calculated M_0 and χ_0 values, the T_c ratio is 0.74 which is within 9% of the measured T_c. This good agreement between theoretical and experimental T_c ratios indicates that the spin-fluctuation theory is a reasonable model for the substitutional modification of these compounds. In our earlier work[24] using the experimental values of M_0 and photoemission results, we concluded that the spin-fluctuation theory did not predict the change in T_c correctly. The discrepancy is due to the difference in the experimental and theoretical values of M_0.

In the next section, the electronic structures of several compounds are measured with photoemission spectroscopy. The relevance of the total (spin-integrated) DOS to the spin-fluctuation model is revealed in Fig. 2 by plotting the exchange-enhanced susceptibility χ_0 as a function of the total DOS at the Fermi energy $N_{tot}(E_F)$ obtained from calculations. The data are taken from previous results on the 2:17 (Ref. 20) and 1:12 (Ref. 21) compounds and the present results on the Mo-substituted compounds. A linear dependence is observed for the Fe-based compounds considered, and the functional form is included on the plot. The parent and nitrided 2:17 compounds are at the limits of the range of values considered, and the change in T_c in the interstitial modification is

FIG. 2. Calculated results of the enhanced susceptibility χ_0 as a function of the total (spin-summed) density of states at the Fermi energy $N_{tot}(E_F)$. The functional form of the linear fit is indicated on the plot.

dominated by the change in the value of χ_0. In contrast, the substitutional modification of $Y_2Fe_{12-x}Mo_x$ shows a relatively small change in χ_0, emphasizing the relative importance of the change in M_0 in the alteration of T_c. As noted previously, T_c increases for Al-substitution in $Sm_2Fe_{17-x}Al_x$ while the magnetization decreases. Using the experimental values of the magnetic moment and T_c for the Al-substituted compounds, the spin-fluctuation theory predicts a dramatic decrease in χ_0 which can be used with Fig. 2 to anticipate a similar decrease in the experimentally measured $N_{tot}(E_F)$. The electronic structure of the Al-substituted compounds have not been calculated because the site of Al substitution has not been uniquely identified.[5,8]

IV. EXPERIMENTAL RESULTS AND DISCUSSION

A. Sample preparation

Bulk samples of $Sm_2Fe_{17-x}Al_xN_y$, $NdFe_{11}TiN_y$, and $Y_2Fe_{12-x}Mo_x$ were prepared by arc melting at least 99.9% pure powders in flowing argon on a water-cooled copper boat. The samples were melted several times to ensure homogeneity. The samples were wrapped separately in Ta foil and annealed in a vacuum of 10^{-6} Torr for several days at temperatures ranging from 850 C to 1100 °C; the details of the vacuum annealing can be found in the literature [Sm_2Fe_{17} (Ref. 12), $NdFe_{11}Ti$ (Ref. 25), $Y_2Fe_{12-x}Mo_x$ (Ref. 10)]. A second Sm_2Fe_{17} sample was prepared by arc melting Sm, Fe, and 4% Nb (by weight) and the vacuum annealing stage was not required to obtain single-phase samples.[26] A portion of each button was pulverized and powder x-ray diffraction verified the proper structure for each compound (rhombehedral Th_2Zn_{17} for the 2:17 compounds and tetragonal $ThMn_{12}$ for the 1:12 compounds). A disk approximately 1.5 cm in diameter and 1 mm thick was spark cut from each button and the surfaces were polished to an optically smooth finish. Scanning electron micrographs of the Sm_2Fe_{17}+Nb sample showed a polycrystalline structure with grain diameters less than 1 μm. X-ray diffraction of the Sm_2Fe_{17}+Nb bulk sample showed that it was textured with the c axis perpendicular to the surface. The texturing may be due to the cooling pattern of the button on the cooled copper boat.[27] The samples were stored in a dessicator to prevent oxidation of the surface prior to insertion in the ultrahigh vacuum system.

The samples were mounted on a tantalum-tungsten manipulator in an ultrahigh-vacuum chamber with a base pressure of 2×10^{-10} Torr. A tungsten heating filament was placed behind the samples for radiative or electron beam heating and the sample temperature was monitored with a type-K thermocouple. The samples were cleaned with Ar ion bombardment, and the surface composition was monitored with Auger electron spectroscopy (AES). The Auger electrons are created by an incident electron beam with an energy of 2.0 keV and a current of 0.2 μA at an angle of 60° to the sample normal.
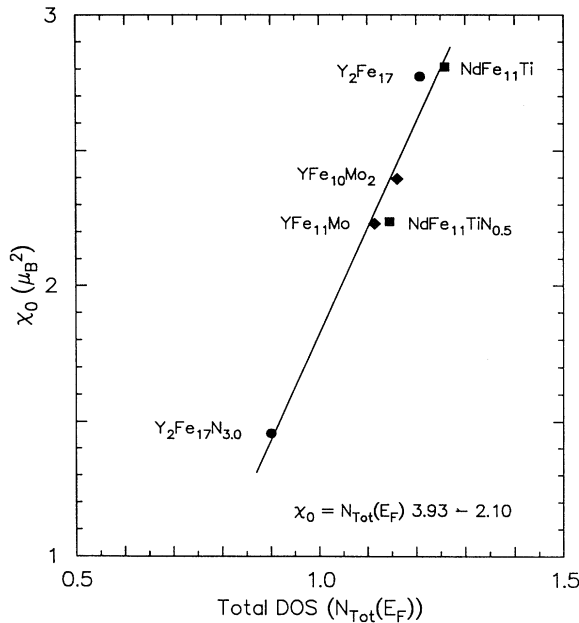
The Auger and photoemitted electrons are analyzed

with a 90° electrostatic sector with a mean radius of 117 mm manufactured by Surface/Interface Inc. The energy-analyzer front-end optics collects electrons emitted within a solid ±20° cone, collimates them with a Pierre electron lens system, and injects them into the energy analyzer. The analyzer is operated in the constant retardation-ratio mode, and the pass energy E_{pass} of the electrons through the 90° sector is one-fourth the initial kinetic energy. The 90° sector is configured as half of a hemispherical analyzer and the electron-energy resolution ΔE is determined by the ratio of the radii of the exit aperture r and the mean radius, $\Delta E/E_{pass} = r(mm)/117$. For the AES data presented below, the exit aperture is 3.5 mm, the spectra are accumulated in the pulse counting mode, the derivative is obtained numerically, and the energy resolution at 400 eV initial kinetic energy (near the nitrogen Auger peak) is 1.28 eV. The photemission data are obtained with an exit aperture of 1.5 mm, and the electron-energy resolution at 19 eV initial kinetic energy is 0.06 eV.

B. Nitrogen addition

A unique method of nitriding was employed in order to maintain the base pressure in the vacuum system. The surface was initially cleaned with several cycles of argon sputtering and annealing to 350 °C, and Auger and photoemission spectra of the parent compound were acquired. Auger spectra obtained during the nitriding process are shown in Fig. 3. The nitrogen ions were implanted with a kinetic energy of 2 keV and a current of 1×10^{-6} amperes for 10 min. The nitrogen ions were generated and accelerated with the same ion sputter gun used for argon sputter cleaning. Using the Auger sensitivity factors[28] and normalizing the Fe to the formula value ($Sm_2Fe_{17}N_x$), the N content is estimated to be $x = 9.8 \pm 0.6$ after implantation. The nitrogen-rich surface region acts as a source of nitrogen for diffusion in subsequent anneals to 400 °C for several minutes. The surface nitrogen concentration is reduced to $x = 3.2 \pm 0.4$ after the sample was annealed in ultrahigh vacuum. The nitrogen-rich surface region is then removed with argon ion sputtering and the subsurface nitride layer was exposed. The nitrogen concentration x was measured as a function of depth with argon ion sputtering and Auger spectroscopy. The subsurface nitrogen concentration was measured as $x = 2.6 \pm 0.4$, and the nitride region was estimated to be 1.4 μm thick. These results are similar to Kerr microscopy observations of the nitrogenation of grains by Mukai and Fujimoto.[29] In their work, a surface-nitrided region approximately 1.5 μm thick is present in grains of Sm_2Fe_{17} after annealing at 500 °C in nitrogen for 1 min.

The $NdFe_{11}Ti$ compound was nitrided using the same method, but unfortunately the Ti Auger line overlaps the N Auger line and an accurate measure of the N concentration in this compound was not obtained. The $YFe_{12-x}Mo_x$ compounds were also nitrided and the Auger spectrum from the nitrided compound is shown in Fig. 3. Normalizing the Fe content to the formula $YFe_{11}MoN_y$ a value of $y = 0.8 \pm 0.4$ was obtained with AES. A similar value of reduced N concentration was observed in Co-based 1:12 compounds.[30] The difference in nitrogen concentration for the two compounds supports the assertion that the bulk atomic structure is present up to the surface which is probed by AES and photoelectron spectroscopy (PES).

C. Photoemission experiments

The electronic structures of the samples were investigated with (PES) experiments carried out at the Synchrotron Radiation Center in Wisconsin. The energy distribution curves (EDCs) of the Sm_2Fe_{17}, $NdFe_{11}Ti$, and $YFe_{12-x}Mo_x$ compounds have been published previously,[24,30,31] and the EDCs are included here with further data analysis on the DOS at E_F as described below. The EDCs of Al-substituted $Sm_2Fe_{17-x}Al_x$ compounds are included as a test of the spin-fluctuation theory. Spin-resolved EDCs from $Sm_2Fe_{17}N_{2.6}$ are compared to the calculated majority and minority DOS.

The photon-energy range used in the spin-integrated experiments was between 18 and 30 eV, and the spectra displayed here were obtained with 22.5 eV. In order to obtain a justifiable measure of the change in the DOS at E_F, $N_{tot}(E_F)$, the EDCs were obtained at several photon energies and the integrated area within several eV of the Fermi energy was normalized to the Fe concentration. Several integration energy ranges were considered, and the range from -0.5 eV to 2.0 eV binding
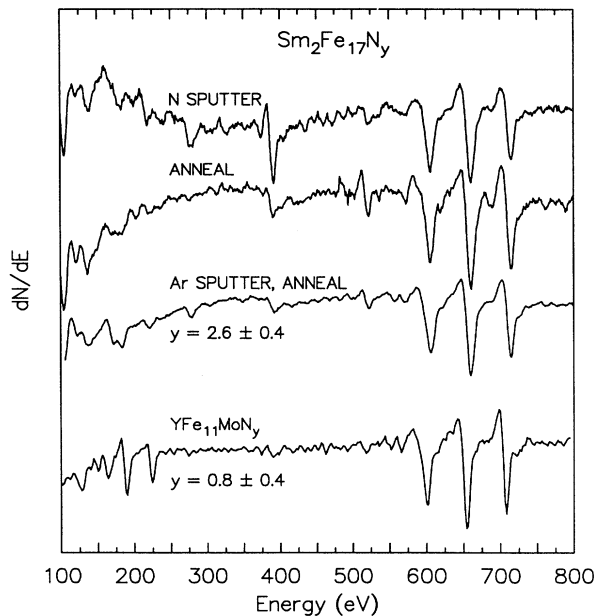

FIG. 3. Auger electron spectra for various steps in the nitriding process for Sm_2Fe_{17}. The nitrogen Auger energy is near 400 eV and the Fe Auger energies are in the range of 600–700 eV. The nitrided Sm_2Fe_{17} is compared to the nitrided $YFe_{11}Mo$.

energy was taken to be dominated by the Fe $3d$ electron emission. $N_{\text{tot}}(E_F)$ values were estimated by fitting the EDCs within ± 0.25 eV of the Fermi energy with a room-temperature Fermi function that was convolved with a Gaussian to represent the instrumental broadening. It is anticipated that the error bars for the data analysis will be substantial due to the difference in the structure

causing a differing matrix element for photoemission and differing electron scattering.

The valence EDCs of the compounds are shown in Figs. 4–7 with calculated electronic structure where available. In all the spectra, the Fe $3d$ band from 0 to 2 eV is readily apparent and the second Fe feature near 2.5 eV binding energy in the calculation is somewhat discernible
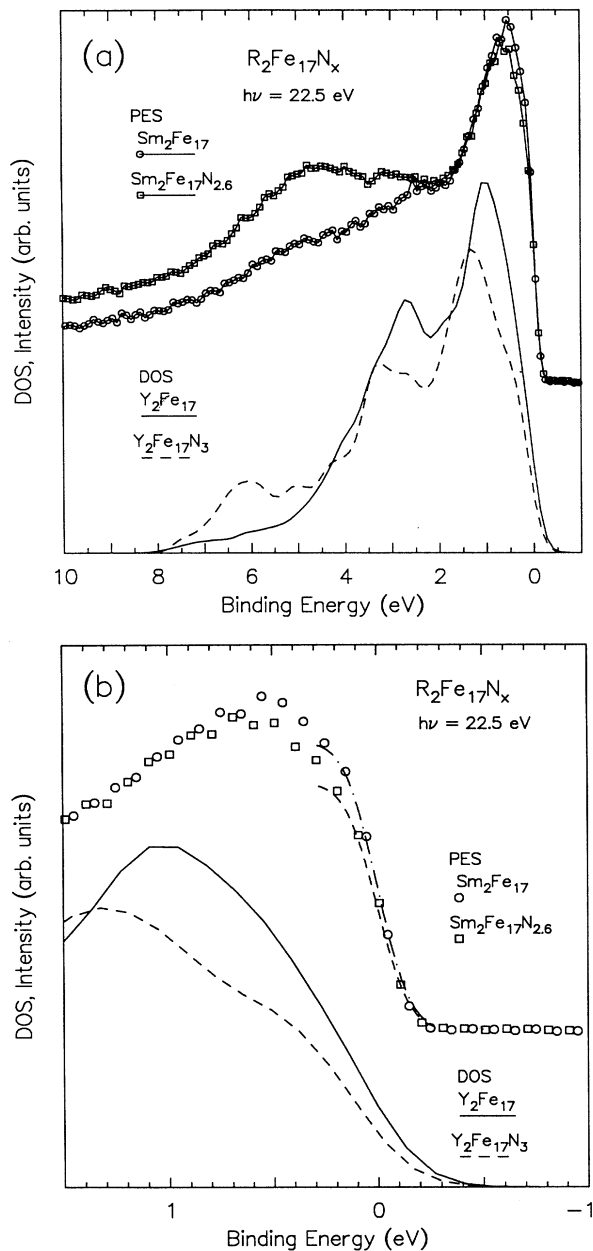

FIG. 4. (a) Upper curves: photoemission spectra for Sm_2Fe_{17} and $Sm_2Fe_{17}N_{2.6}$ normalized as described in the text. Lower curves: calculated density of states for Y_2Fe_{17} and $Y_2Fe_{17}N_3$. (b) Same data as in (a) with an expanded binding energy scale in the neighborhood of the Fermi energy. The dot-dashed and dashed lines on the experimental data are the fit of the convoluted Fermi function to the Fermi edge.
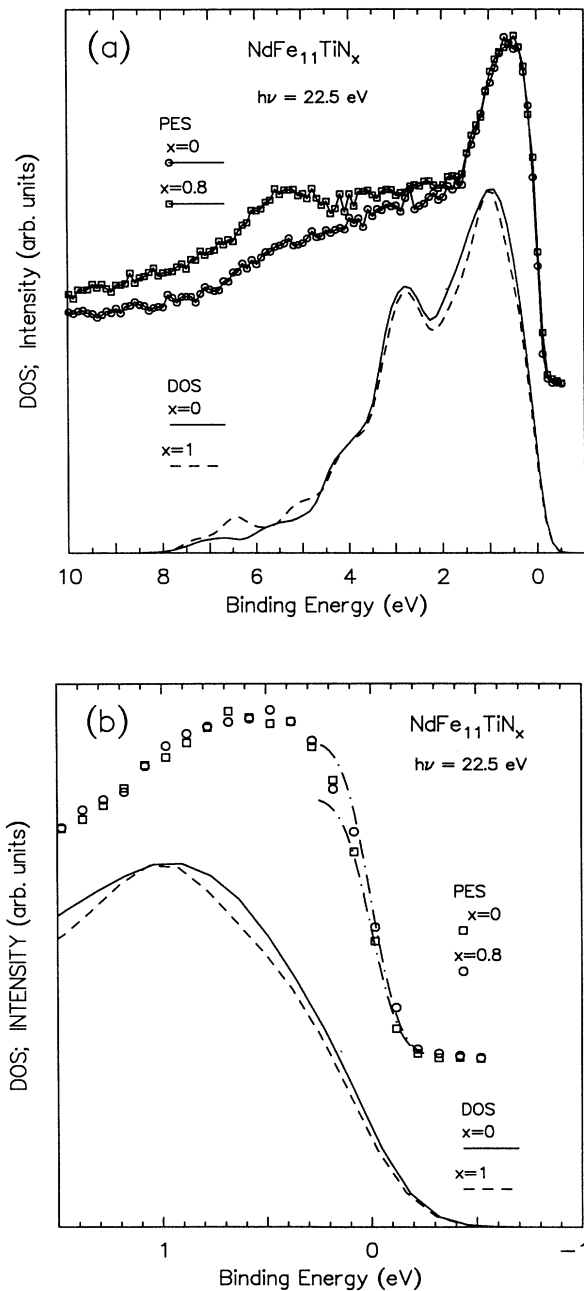
FIG. 5. (a) Upper curves: Photoemission spectra of $NdFe_{11}Ti$ and $NdFe_{11}TiN_{0.8}$. Lower curves: calculated density of states for the same compounds as noted. (b) Same data as in (a) with an expanded binding energy scale in the neighborhood of the Fermi energy. The dot-dashed lines are $\pm$ 10% of the best fit of the convoluted Fermi function.

in the EDCs. The change in the $3d$ bandwidth, an expected narrowing as the moment increases, cannot be discerned with the EDCs. The contribution due to nitrogen is observed in Figs. 4 and 5 at ~ 5 eV, and the binding energy in the EDC is substantially lower than the calculated nitrogen binding energy. The most sub-

stantial difference between the EDCs and the calculated DOS is that the EDC is a measure of a photoionized state which includes photoemission matrix elements, lifetime broadening, electron transport, and secondary electron phenomenon. The calculated DOS represents the ground state of the electronic structure and there is fair
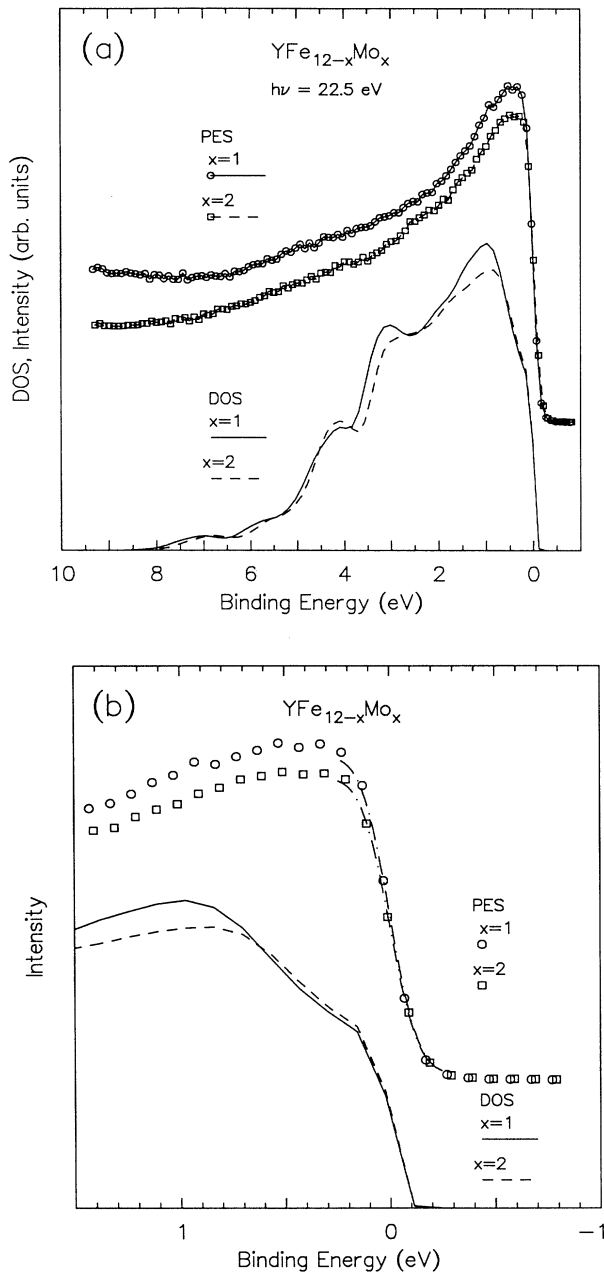

FIG. 6. (a) Upper curves: photoemission spectra for $YFe_{11}Mo$ and $YFe_{10}Mo_2$ normalized as described in the text. Lower curves: calculated density of states for $YFe_{11}Mo$ and $YFe_{10}Mo_2$. (b) Same data as in (a) with an expanded binding energy scale in the neighborhood of the Fermi energy. The dot-dashed lines on the experimental data are the fit of the convoluted Fermi function to the Fermi edge.
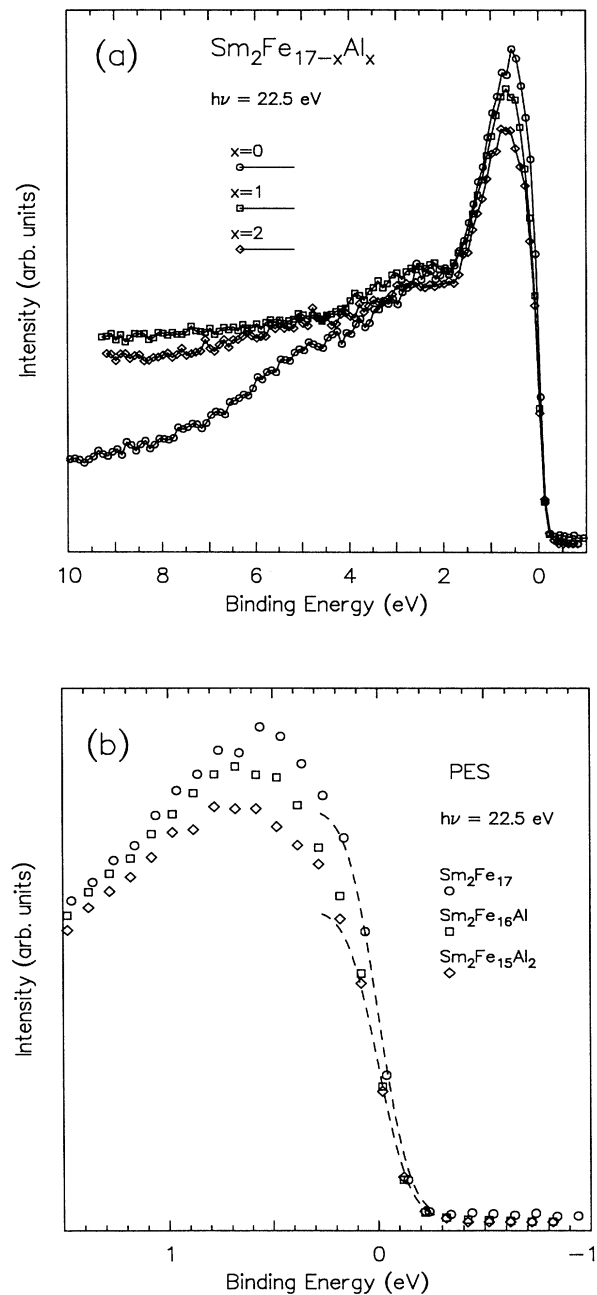
FIG. 7. (a) Photoemission spectra for $Sm_2Fe_{17-x}Al_x$ with $x = 0, 1, 2$. (b) Same data as in (a) with an expanded binding energy scale in the neighborhood of the Fermi energy. The dashed lines are the best fit of the convoluted Fermi function to the Fermi edge.

agreement between the calculated DOS and the measured EDCs.

The lifetime broadening is due to the lifetime of the photocreated empty state; the larger the lifetime, the smaller the broadening. Models of the lifetime broadening generally assume that the lifetime is proportional to $(E_B - E_F)^2$, where E_B is the binding energy. The lifetime is roughly determined by the number of states (with lower binding energy) available to fill the empty state, and the broadening at E_F is generally assumed to be zero. The states at E_F have a long lifetime, and the EDC at E_F can be taken as a measure of the DOS at E_F. The EDCs and calculated DOS within 1.5 eV of the Fermi energy are shown in Figs. 4(b)–7(b). In all the figures, the experimental Fermi edge is sharper than the calculated edge which has been broadened by a Gaussian to simulate instrumental response, and the peak position of the $3d$ EDC bands occur at a substantially lower binding energy than the calculated $3d$ DOS bands. Qualitatively the change in the EDCs in Figs. 4(b)–7(b) agree with the change in the calculated DOS. In Fig. 5(b), the upper and lower dot-dashed curves at E_F are ± 10% error bars of the best fit to both sets of EDCs. The error for each individual EDC is estimated as ± 8% and the ratio of the EDCs at E_F will include an error of ± 16%. In all cases the EDCs and the DOS decrease as T_c increases within experimental error. Quantitatively, the results of the fitting of the convoluted Fermi functions are given in Table I and compared to the calculated results. The relative change of the EDCs and the DOS for both nitrogen interstitial and substitutional modifications are in very good agreement, within the limit of the experimental error.

In Fig. 7(b) the modifications of the EDCs at E_F are shown with the fitted convoluted Fermi function. The measured EDC at E_F can be used with the enhanced susceptibility curve in Fig. 2 and the experimentally measured M_0 values to determine a ratio in T_c for Al substitution which can be compared to experimentally determined T_c ratio. The T_c ratio determined by the spin-fluctuation model can be written

$$\frac{T_c(x=2)}{T_c(x=0)} = \left(\frac{M_0(x=2)}{M_0(x=0)}\right)^2 \frac{\chi_0(x=0)}{\chi_0(x=2)} , \qquad (4)$$

TABLE I. Ratios of the calculated density of states at the Fermi energy and the fitted experimental energy distribution curve at the Fermi energy.

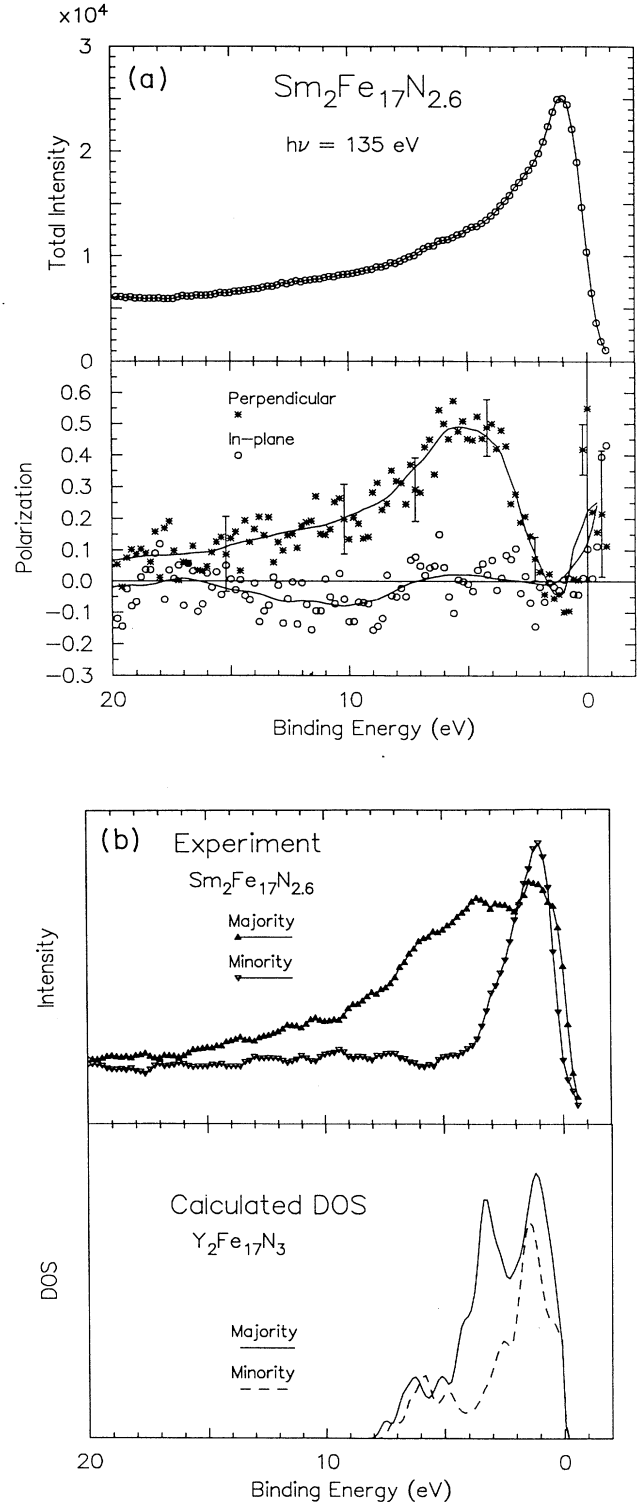| Compounds	Calculation	Experiment (error ±0.16)
$\frac{R_2Fe_{17}N_3}{R_2Fe_{17}}$	0.75	0.85
$\frac{NdFe_{11}TiN}{NdFe_{11}Ti}$	0.91	1.0
$\frac{YFe_{11}Mo}{YFe_{10}Mo_2}$	0.96	1.07
$\frac{Sm_2Fe_{15}Al_2}{Sm_2Fe_{17}}$		0.75

FIG. 8. (a) Spin-resolved photoemission of Sm_2Fe_{17} obtained with a photon energy of 135 eV showing the total intensity and the measured perpendicular and in-plane components of the polarization as a function of binding energy using a Sherman function of 0.05. (b) Comparison of the experimental and calculated majority- and minority-spin EDCs in the perpendicular orientation.

where x is the aluminum content, the zero-temperature moments are $M_0(0) = 35.2\mu_B/$f.u., and $M_0(2) = 27.4\mu_B/$f.u. The enhanced susceptibility for the Y_2Fe_{17} compound from Ref. 20 and plotted in Fig. 2 is $\chi_0(0) = 2.77\mu_B^2$. Using this value with the change in EDCs at E_F in Fig. 7(b), the enhanced susceptibility for $x = 2$ is $\chi_0(2) = 1.55\mu_B^2$. The experimentally determined ratio of the T_c values is 1.16,[8] and using the above determined parameters the spin-fluctuation theory predicts a ratio of

$$\frac{T_c(2)}{T_c(0)} = \left(\frac{27.4}{35.2}\right)^2 \frac{2.77}{1.55} = (0.61)(1.79) = 1.09 , \quad (5)$$

which is within 6% of the experimentally determined T_c ratio. Thus the spin-fluctuation model predicts the T_c change of the substitutionally modified compound very well.

D. Spin-resolved photoemission

Spin-resolved photoemission of the $Sm_2Fe_{17}N_{2.6}$ valence band was obtained with a higher-intensity and higher-energy (135 eV) photon beam on the Mark V monochromator at the synchrotron. The photon energy is below the Sm $4d \rightarrow 4f$ resonance, and the EDC is dominated by the Fe $3d$ electrons. A diffuse-scattering spin analyzer with a Sherman function of 0.05 (Ref. 32) is used to measure two components of the photoelectron spin perpendicular and parallel to the surface. The Sm_2Fe_{17} sample was mounted on a magnetic core and a magnetic field was applied to the sample. After nitriding the sample, the c axis is the easy axis of magnetization and the polarizations perpendicular and parallel to the surface are presented in Fig. 8(a) with the total intensity. The statistical error is shown at several points on the polarization curves and the solid line is determined by a smoothing of the raw data and is intended to serve as a guide to the eye. The data are obtained from two EDCs from the four anodes in the spin analyzer and the instrumental asymmetry is removed using the data analysis described by Kessler.[33] The in-plane component of polarization is zero within the statistical error, and the perpendicular polarization shows significant structure in the valence band. The polarization spectra show that the material is magnetized perpendicular to the surface which agrees with previous determination of the magnetic anisotropy of the nitrided Sm_2Fe_{17} compounds.

The perpendicular polarized majority- and minority-spin components of the spectra obtained from the polarization and intensity data are shown in Fig. 8(b) with

the spin-resolved DOS calculation.[20] The minority-spin experimental data show a good agreement with the calculation and the majority-spin data exhibit a broad feature, and the net polarization is positive for binding energies up to 18 eV. The spin-resolved spectra in Fig. 8 near the Fermi energy show that the polarization is positive at E_F in excellent agreement with the spin-resolved calculated DOS shown in the figure. In previous spin-resolved PES spectra from pure iron samples,[34] the polarization is dominated by minority-spin electrons within 1 eV of the Fermi energy.

V. CONCLUSIONS

The spin-fluctuation T_c theory of Mohn and Wohlfarth has been applied to both interstitial and substitutional modifications of the 2:17 and 1:12 R-T compounds. The theory and experimental data support the spin-fluctuation model of T_c as the model correctly predicts the change in T_c as the compound is modified. From the calculated electronic structures, the enhanced susceptibility χ_0 is linearly related to the total (spin-summed) DOS at E_F. This result has been applied to determine the change in T_c of the Al-substituted $Sm_2Fe_{17-x}Al_x$ compound with very good agreement between the model and the measured T_c change. Spin-resolved photoemission spectra from Sm_2Fe_{17} have shown that the magnetization is perpendicular to the surface and the spin-resolved electronic structure agrees with the calculated DOS. The T_c modification of the Fe-based R-Fe compounds have been well modeled with the spin-fluctuation model. Substitutional alloying or interstitial nitriding or carbiding of the parent binary or ternary compounds has important practical implications in certain cases for permanent-magnet materials. The understanding achieved in the present series of measurements and calculations is a first step in developing a more detailed understanding based on local-environment effects, moment instabilities, and spin-polarized disordered alloying effects. These considerations will be important for future studies of these and related materials.

ACKNOWLEDGMENTS

[1] J. F. Herbst, Rev. Mod. Phys. **63**, 819 (1991), and references therein.

[2] K. J. Strnat, in *Ferromagnetic Materials*, edited by E. P. Wohlfarth and K. H. J. Buschow (North-Holland, Amsterdam, 1989), Vol. 4, p. 131.

[3] K. H. J. Buschow, in *Ferromagnetic Materials*, edited by E. P. Wohlfarth and K. H. J. Buschow (North-Holland, Amsterdam, 1986), Vol. 1, p. 297.

[4] J. M. D. Coey and H. Sun, J. Magn. Magn. Mater. **87**, L251 (1990); H. Sun, J. M. D. Coey, Y. Otani, and D. P. R. Hurley, J. Phys. Condens. Matter **2**, 6465 (1990).

[5] D. McNeely and H. Oesterreicher, J. Less-Common Met. **44**, 183 (1976).

[6] T. H. Jacobs, K. H. J. Buschow, G. F. Zhou, X. Li, and F.

R. de Boer, J. Magn. Magn Mater. **116**, 220 (1992).

[7] Bo-Ping Hu, Xiao-Lei Rao, Jian-Min Xu, Gui-Chuan Liu, Fei Cao, Xiao-Lin Dong, Hua Li, Lin Yin, and Zhong-Ren Zhao, J. Magn. Magn. Mater. **114**, 138 (1992).

[8] Z. Wang and R. A. Dunlap, J. Phys. Condens. Matter **5**, 2407 (1993).

[9] J. M. D. Coey, in *Ferromagnetic Materials*, edited by E. P. Wohlfarth and K. H. J. Buschow (North-Holland, Amsterdam, 1991), Vol. 6, p. 1.

[10] Hong Sun, M. Akayama, K. Tatami, and H. Fujii, Physica B **183**, 33 (1993).

[11] D. B. de Mooij and K. H. J. Buschow, J. Less-Common. Met. **136**, 207 (1988).

[12] Hong Sun, J. M. D. Coey, Y. Otani, and D. P. F. Hurley, J. Phys. Condens. Matter **2**, 6465 (1990).

[13] Qi-nuan Qi, Hong Sun, R. Skomski, and J. M. D. Coey, Phys. Rev. B **45**, 12 278 (1992).

[14] M. Katter, J. Wecker, L. Schultz, and R. Grossinger, J. Magn. Magn. Mater. **92**, L14 (1990).

[15] P. Mohn and E. P. Wohlfarth, J. Phys. F **17**, 2421 (1987).

[16] John B. Goodenough, *Magnetism and the Chemical Bond* (Interscience, New York, 1963), pp. 78–80.

[17] Chih-Wen Chen, *Magnetism and Metallurgy of Soft Magnetic Materials* (Dover, New York, 1986).

[18] D. P. Middleton and K. H. J. Buschow, J. Alloys Compounds **206**, L1 (1994).

[19] E. P. Wohlfarth, Phys. Lett. **3**, 17 (1962).

[20] S. S. Jaswal, W. B. Yelon, G. C. Hadjipanayis, Y. Z. Wang, and D. J. Sellmyer, Phys. Rev. Lett. **67**, 644 (1991).

[21] S. S. Jaswal, Phys. Rev. B **48**, 6156 (1993).

[22] H. K. Skriver, in *The LMTO Method*, edited by M. Cardona,

P. Fulde, and H.-J. Queisser, Springer Series in Solid State Sciences Vol. 41 (Springer-Verlag, New York, 1984).

[23] M. Katter, J. Wecker, C. Kuhurt, L. Schultz, and R. Grossinger, J. Magn. Magn. Mater. **114**, 35 (1992).

[24] A. S. Fernando, J. P. Woods, S. S. Jaswal, B. M. Patterson, D. Welipitiya, and D. J. Sellmyer, J. Appl. Phys. **75**, 6303 (1994).

[25] B.-P. Hu, H.-S. Li, J. P. Gavigan, and J. M. D. Coey, J. Phys. Condens. Matter **1**, 755 (1989).

[26] A. E. Platts, I. R. Harris, and J. M. D. Coey, J. Alloys Compounds **185**, 251 (1992).

[27] J. M. D. Coey (private communication).

[28] Lawerence E. Davis, Noel C. MacDonald, Paul W. Palmberg, Gerald E. Riach, and Roland E. Weber, *Handbook of Auger Electron Spectroscopy* (Perkin Elmer, Eden Prairie, MN, 1978).

[29] Toshio Mukai and Tatsuo Fujimoto, J. Magn. Magn. Mater. **103**, 165 (1992).

[30] A. S. Fernando, J. P. Woods, S. S. Jaswal, B. M. Patterson, D. Welipitiya, A. S. Nazareth, and D. J. Sellmyer, J. Appl. Phys. **73**, 6919 (1993).

[31] J. P. Woods, A. S. Fernando, S. S. Jaswal, B. M. Patterson, D. Welipitiya, and D. J. Sellmyer, J. Appl. Phys. **73**, 6913 (1993).

[32] D. G. Van Campen, R. J. Pouliot, and L. E. Klebanoff, Phys. Rev. B **48**, 17 533 (1993).

[33] Joachim Kessler, *Polarized Electrons* (Springer-Verlag, New York, 1985), p. 234.

[34] E. Kisker, in *Spin- and Angle-Resolved Photoemission from Ferromagnets*, edited by R. Feder (World Scientific, Singapore, 1985).